

# High Strains Near Femoral Insertion Site of the Superficial Medial Collateral Ligament of the Knee Can Explain the Clinical Failure Pattern

Thomas Luyckx,<sup>1</sup> Matthias Verstraete,<sup>2</sup> Karel De Roo,<sup>2</sup> Catherine Van Der Straeten,<sup>2</sup> Jan Victor<sup>2</sup>

<sup>1</sup>Department of Orthopaedic Surgery, University Hospitals Leuven, Leuven, Belgium, <sup>2</sup>Department of Orthopaedic Surgery and Traumatology, University Hospital Ghent, Ghent, Belgium

Received 17 October 2014; accepted 23 February 2016

Published online in Wiley Online Library (wileyonlinelibrary.com). DOI 10.1002/jor.23226

**ABSTRACT:** The three dimensional (3D) deformation of the superficial medial collateral ligament (sMCL) of the knee might play an important role in the understanding of the biomechanics of sMCL lesions. Therefore, the strain and deformation pattern of the sMCL during the range of motion were recorded in five cadaveric knees with digital image correlation. During knee flexion, the sMCL was found to deform in the three planes. In the sagittal plane, a rotation of the proximal part of the sMCL relative to the distal part occurred with the center of this rotation being the proximal tibial insertion site of the sMCL. This deformation generated high strains near the femoral insertion site of the sMCL. These strains were significantly higher than in the other parts and were maximal at 90° with on average +3.7% of strain and can explain why most lesions in clinical practice are seen in this proximal region. The deformation also has important implications for sMCL reconstruction techniques. Only a perfect anatomic restoration of the insertion sites of the sMCL on both the proximal and distal tibial insertion sites will be able to reproduce the isometry of the sMCL and thus provide the adequate stability throughout the range of motion. The fact that knee motion between 15° and 90° caused minimal strain in the sMCL might suggest that early passive range of motion in physical therapy postoperatively should have little risk of stretching a graft out in the case of an anatomical reconstruction. © 2016 Orthopaedic Research Society. Published by Wiley Periodicals, Inc. *J Orthop Res*

**Keywords:** knee; isometry; medial collateral ligament; stability; MCL reconstruction

As the primary static stabilizer preventing valgus rotation, the medial collateral ligament is one of the most frequently injured ligaments of the knee.<sup>1–3</sup> The incidence of these injuries has been reported to be as high as 0.24 per 1,000 in the United States in any given year.<sup>4</sup> The mechanism of injury involves valgus stress, usually combined with an external tibial rotation component from either a noncontact (pivoting or cutting) or a contact injury (direct blow to the lateral side of the knee) in slight knee flexion.<sup>2</sup> The majority of medial collateral ligament tears are isolated. Studies have reported that most of the lesions are located near the femoral insertion site.<sup>5,6</sup>

Historically, the treatment of acute medial collateral ligament injuries has mainly focused on conservative measures, reporting good outcomes. More recently, the repair and reconstruction of more severe acute grade III and symptomatic chronic medial collateral ligament injuries has gained interest.<sup>7,8</sup> The concept of ligament isometry has been at the heart of models that describe normal knee motion and is crucial for anatomic superficial medial collateral ligament (sMCL) reconstruction techniques.<sup>9,10</sup> The sMCL is an isometric ligament in its central fibers although previous work showed a different behavior described between the anterior and posterior part of the sMCL.<sup>11,12</sup> A ligament is generally considered isometric when the change in length and thus the strain in the whole ligament during the arc of motion is less than 2%.<sup>10,13</sup> Whether a 2% strain should be considered minimal is a question that can be raised because

studies have reported that damage accumulation in the collagen fibers may already start at four or 5% strain.<sup>14</sup> Moreover, at local areas of the sMCL, a different situation may exist because biological tissue is inhomogeneous, non-linear and anisotropic. Strain propagation and distribution in the ligament may therefore demonstrate important regional variation. Previous studies have reported significant differences in forces and strains between the proximal versus the distal part and the anterior versus the posterior part of the sMCL.<sup>11,12,15</sup> However, in most studies, the forces defining different regions were very rough and the strain measurement techniques lacked resolution and accuracy.<sup>11,15</sup> The strain gauges that were used require an amount of dissection for their insertion and require some form of fixation to the tissue thereby potentially introducing measurement errors.<sup>16</sup> Moreover, they act as point gauges and thus fail to show regional strain patterns. In this study, three dimensional (3D) digital image correlation (DIC) was therefore adopted to investigate the strain distribution in the sMCL of the knee.

The purpose of the study was to describe the strain and the deformation of the sMCL of the knee during loaded knee motion by creating a high-resolution 3D strain map and to analyse sub-regional strain differences. It was hypothesized that the sMCL would behave isometrically (<2% strain), that the sub-regional (<1 cm<sup>2</sup>) strain would be inhomogeneously distributed over its surface and that deformation would be minimal.

## MATERIALS AND METHODS

Six paired fresh frozen lower limbs, disarticulated at the level of the hip, were obtained from two male and one female human donors after approval of the study protocol by Ethics committee. The donors were 48, 69, and 70 years of age when they died. Demographic data of the specimens can be

Conflict of interest: None.

Grant sponsor: University of Ghent.

Correspondence to: Thomas Luyckx (T: +3216338070; F: +32473967200; E-mail: luyckx.thomas@gmail.com)

© 2016 Orthopaedic Research Society. Published by Wiley Periodicals, Inc.

found in Table 1. The specimens were stored at  $-22^{\circ}\text{C}$  prior to the experiment.

For all six knee specimens, CT images were obtained with a volumetric CT scanner (Toshiba Medical Systems, Otawara, Japan). The slice thickness was 0.5 mm, the image matrix was  $512 \times 512$  pixels and the pixel size was 0.625 mm. The CT scans were performed with the specimens in the frozen state to preserve the quality of the specimens. Each knee was assessed for abnormalities. Exclusion criteria were: Previous surgery on the knee, previous trauma of the cruciate ligaments or significant osteoarthritis. One specimen had a degenerative medial meniscal tear with a parameniscal cyst. However, the integrity of the sMCL was not compromised. All CT scans were uploaded in a three-dimensional visualization software system (Mimics 14.12, Materialise, Haasrode, Belgium) for further analysis. After a bone surface reconstruction mask was created, all relevant surface landmarks and ligament insertion sites on the medial side of the knee were identified based on the quantitative descriptions of LaPrade<sup>17</sup> and Victor.<sup>10</sup> These data were combined with the 3D-DIC data to add surface anatomy to the analysis.

Prior to dissection, the specimens were thawed overnight at a room temperature of  $20^{\circ}\text{C}$  and prepared by resecting the skin and subcutaneous fat. Meticulous prevention of drying out of the specimen was done throughout the experiment by using wet towels and water spraying. The femur was severed 35 cm proximal to the knee joint line and 20 cm of bone was cleared from soft tissue for embedding. The tibia was severed 28 cm distal to the knee joint line and all soft tissues were cleared from the bone 5 cm distally to the distal tibial sMCL insertion site. The femur was rigidly fixed in a cylindrical container using a polyester resin.

Next, the sMCL was anatomically prepared. The sartorius, semitendinosus, and gracilis tendons were removed from their attachment sites to allow adequate visualization of the distal sMCL. The proximal and distal insertion sites of the sMCL were identified according to the quantitative anatomical description by LaPrade.<sup>17</sup> The sMCL was left untouched in its native bed. Next, all muscle attachment sites of the different parts of the quadriceps (vastus medialis obliquus [VMO], vastus medialis longus [VML], vastus intermedius [VI], rectus femoris [RF], vastus lateralis longus [VLL], and vastus lateralis obliquus [VLO]), the semimembranosus (SM), the biceps femoris and the iliotibial band were located and Ethibond 2 suture (Ethicon, Johnson and Johnson, Somerville, New Jersey) loop was attached to these muscles to provide an anchor for applying load in the knee rig.

The construct was mounted in a custom made knee rig based on the work of Amis et al.<sup>18</sup> The set-up consisted of a framework in which the cylindrical container of the femur was rigidly fixed. The tibia was left unconstrained, allowing six degrees of freedom in the knee. A total load of 175 N was proportionately divided over the different parts of the quadriceps muscle, 30 N was applied to the iliotibial band (ITB) and 50 N to the medial and lateral hamstrings (Fig. 1). The load was applied according to the cross-sectional areas of each

muscle unit, based on the work of Farahmand et al.<sup>19</sup> and Victor et al.<sup>20</sup> The load was applied in physiological directions of each muscle by attaching a series of calibrated weights. The direction of the traction cables in the three planes was controlled using a digital inclinometer for each specimen. As a result, a statically balanced muscle loading of the knee was obtained.

Starting from a neutral position with all loads attached, the knee was first brought from the neutral position (on average  $6^{\circ}$  of flexion) to full extension ( $0^{\circ}$ ). Subsequently, the knee was flexed up to  $120^{\circ}$  at  $15^{\circ}$  intervals. The deformation of the sMCL during this movement was recorded through a three-dimensional Digital Image Correlation (DIC) system (Limes GmbH, Pforzheim, Germany). DIC is an optical method for strain measurement that uses image recognition to analyze and compare digital images acquired from the surface of a substrate instead of surface markers. By tracing a randomly applied high contrast speckle pattern using white light, displacement and strain within the specimen can be calculated from subsequent images. The initial imaging processing defines unique correlation areas known as macro-image facets, typically 15–30 pixels square, across the entire imaging area. Each facet is a measurement point that can be thought of as an extensometer point and strain rosette. These facets are tracked in each successive image. Through interpolation and the overlap of adjacent facets, sub-pixel accuracy is obtained in terms of displacement from which the strains can subsequently be calculated. Using one camera only allows for single plane measurements (2D). In this setup, out of field displacement can cause significant error. Transition to the use of two cameras enables three-dimensional (3D) deformation analysis of the whole area of interest and has overcome this error. As with stereopsis, the use of the 2 different images of the same object and the photogrammetric principles enable the calculation of the precise 3D coordinates of each point of the entire surface. In this way, a high-resolution 3D map with strain magnitude, gradient and distribution of the entire study object can be obtained.<sup>21</sup> The experimental setup consisted in this article of two charge-coupled device (CCD) cameras with a resolution of  $2486 \times 1985$  pixels. At each flexion angle, these cameras captured three images of the sMCL. To obtain an optimal contrasted image, the sMCL was prepared with a modified technique as previously published.<sup>22</sup> This implied the application of random white speckle pattern using a water-based white paint in a spray can on the sMCL that was first dyed dark blue with the use of methylene blue. A dedicated software package (VIC3D, Correlated Solutions Inc., Columbia, SC) was used to analyze the deformation and strain at each flexion angle using the camera images.

Both the overall ligament strains and the regional strains in the ligament were measured with the system. A previously reported accuracy analysis reported a low scatter (0.03%) and a high spatial resolution of  $0.1 \text{ mm}^2$  for strain measurement on the Achilles tendon.<sup>22</sup> The accuracy was determined in terms of scatter in the strain measurements between subsequently taken images of the speckled surface in the preloaded condition. This was done in two ways. First, the difference between the minimum and maximum strain in the overall field was evaluated. Second, the scatter in the center-most part of the specimen was evaluated. The second method was applied to overcome disturbing effects from the boundaries of the analyzed area, because it is well known that the correlation is less accurate at the edges. It was concluded that the scatter was low for all specimens; in the

**Table 1.** Demographic Data of the Specimens

Donor nr	Sex	Age	Weight (kg)
Donor A	Male	48	64
Donor B	Male	69	90
Donor C	Female	70	40

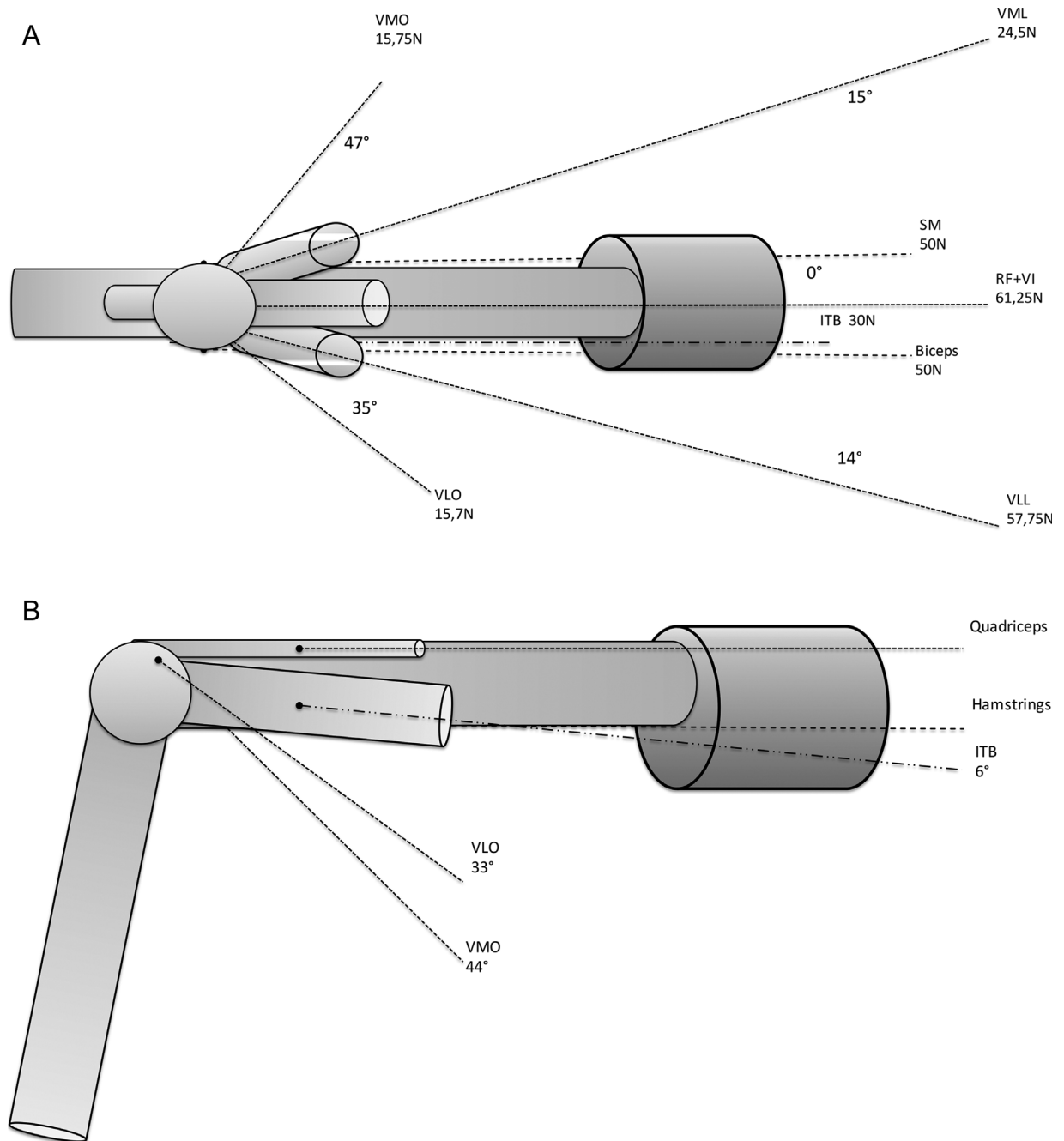


**Figure 1.** Schematic representation of the test setup. A top view is shown on the left side (A) and a view from the side on the right side (B). The pulling direction and the forces for each muscle division are given.

center of the specimens strain values  $\leq 0.2\%$  were obtained, based on a 95% confidence interval and assuming a normal distribution. It is noted that the standard deviation of the strains in the specimen is of the same order of magnitude as for the analyzed areas located on the steel blocks. The spatial resolution was calculated to be  $0.1 \text{ mm}^2$ . From the full field measurements, the strain was evaluated at every tracked point of the sMCL. The longitudinal strain was defined as the strain along the longitudinal axis of the sMCL, from femoral till distal tibial insertion site. Transverse strain was the strain along an axis perpendicular to the longitudinal axis. And shear strain was defined as strain along an axis angulated at  $45^\circ$  to the longitudinal and transverse axis. In

one specimen, the quality of the speckle pattern was insufficient to perform the detailed analysis and it was subsequently excluded from further analysis. Throughout the range of motion, the strain was evaluated as the difference in absolute strain between a given flexion angle and the ligament strain at  $0^\circ$  knee flexion. Isometry was thereby defined as a strain not exceeding 2% with respect to the reference condition ( $0^\circ$  knee flexion).

For the subdivision in the different regions of the sMCL (proximal vs. middle vs. distal), the CT data and the quantitative description of LaPrade were utilized.<sup>17</sup> The distance from the medial epicondyle to the joint line was determined for each specimen. The proximal region was then

defined as the region from the insertion site until 1 cm proximal to the joint line. The middle region was outlined as the region from 1 cm above the joint line until 1.5 cm below. And the distal region was the region from 1.5 cm distal from the joint line until the distal tibial insertion site 6 cm below the joint line.<sup>17</sup>

### Deformation Analysis

From the deformation analysis in the sagittal plane, it was observed that at 60° of flexion, the sMCL was no longer a rectangular bar. A kink was observed at the proximal tibial plateau. The location of this kink was plotted on the pre-operative CT scan using Mimics 14.12 (Materialise, Haasrode, Belgium). To quantitatively evaluate this rotation for all specimens, the deformation of an initial straight line was therefore monitored and, using a least square fit, approximated by a bi-linear fit. The angle between both linear parts of this curve fit, denoted as  $\alpha$ , was subsequently calculated.

### Cumulative Strain Distribution

To overcome the practical issues with the analysis of the data due to the local heterogeneity of the different strain maps, a cumulative strain distribution was created. To that extent, the analyzed area was subdivided in squares of  $1 \times 1$  mm and the strain was evaluated at the center of each square. Subsequently, a cumulative distribution for the whole tendon was calculated from each frame. A typical example of the cumulative strain distribution is shown in Figure 6. The X-axis represents the percentage of the surface area of sMCL. The Y-axis represents strain. In this way, the relative surface area showing a strain of less than and equal to a certain strain was plotted. For example, for specimen 6, at 45° of flexion, 80% of the surface area of the sMCL had a strain less than or equal to 0%. The area under the curve represents a measure for the strain accumulated over the whole sMCL at a certain flexion angle.

### Statistical Analysis

The results from the deformation analysis were tested for normality and were analyzed using a Student's paired *t*-test. The result from the longitudinal strain analysis were analyzed using the Kruskal–Wallis test for multiple comparison (four groups: distal, middle, proximal, and whole sMCL). Post hoc testing was performed by the Wilcoxon rank sum test with Bonferroni adjustments. *p*-values smaller than 0.05 were considered significant. All analyses were performed using SAS software, version 9.2 of the SAS System for Windows (SAS Institute Inc., Cary, NC).

## RESULTS

### Morphology and Deformation Analysis

The total length, as measured from the proximal to distal attachment, and the width of the sMCL as calculated from the 3D DIC analysis was on average 104.1 mm (SD 15.2) and 17.3 mm (SD 3.3), respectively. The three-dimensional morphology of the sMCL was observed with the use of 3D DIC. A characteristic 3D morphology image of the sMCL in extension is shown in Figure 1. In the sagittal plane, an S-shaped morphology was observed. During knee flexion, the sMCL did not behave as a rigid bar but was deformed in three planes. Most deformation occurred in the frontal (XZ) and sagittal (XY) plane (Fig. 2). In the sagittal plane, this deformation was observed at larger flexion angles (beyond 60°) and could be described as a rotation of the proximal part of the sMCL relative to the distal part with the center of this rotation being the proximal tibial insertion site of the sMCL. The angle between both linear parts of a curve fit was denoted as  $\alpha$ . On average, the deformation angle remained close to zero up to a flexion angle of 60 degrees (Fig. 3). Beyond this flexion angle, a significant increase of the deformation angle was

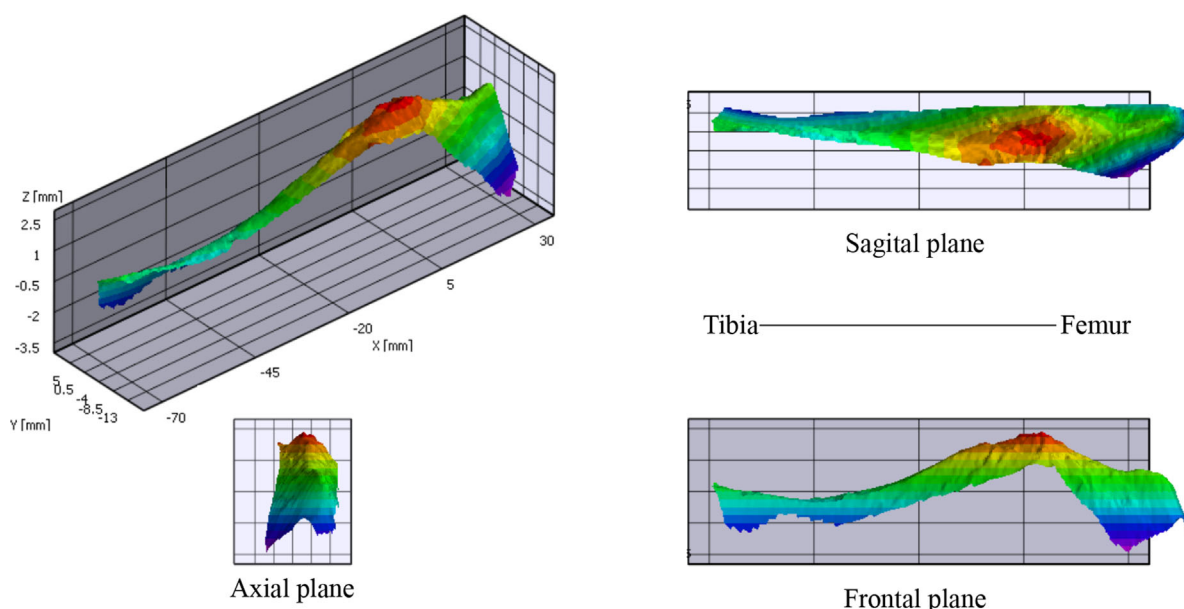


**Figure 2.** 3D morphology of the sMCL at rest position (approx. 6° flexion) showing the Z-coordinate in the colour scale (specimen 3). XY-plane = sagittal plane; XZ-plane = frontal plane; YZ-plane = axial plane.

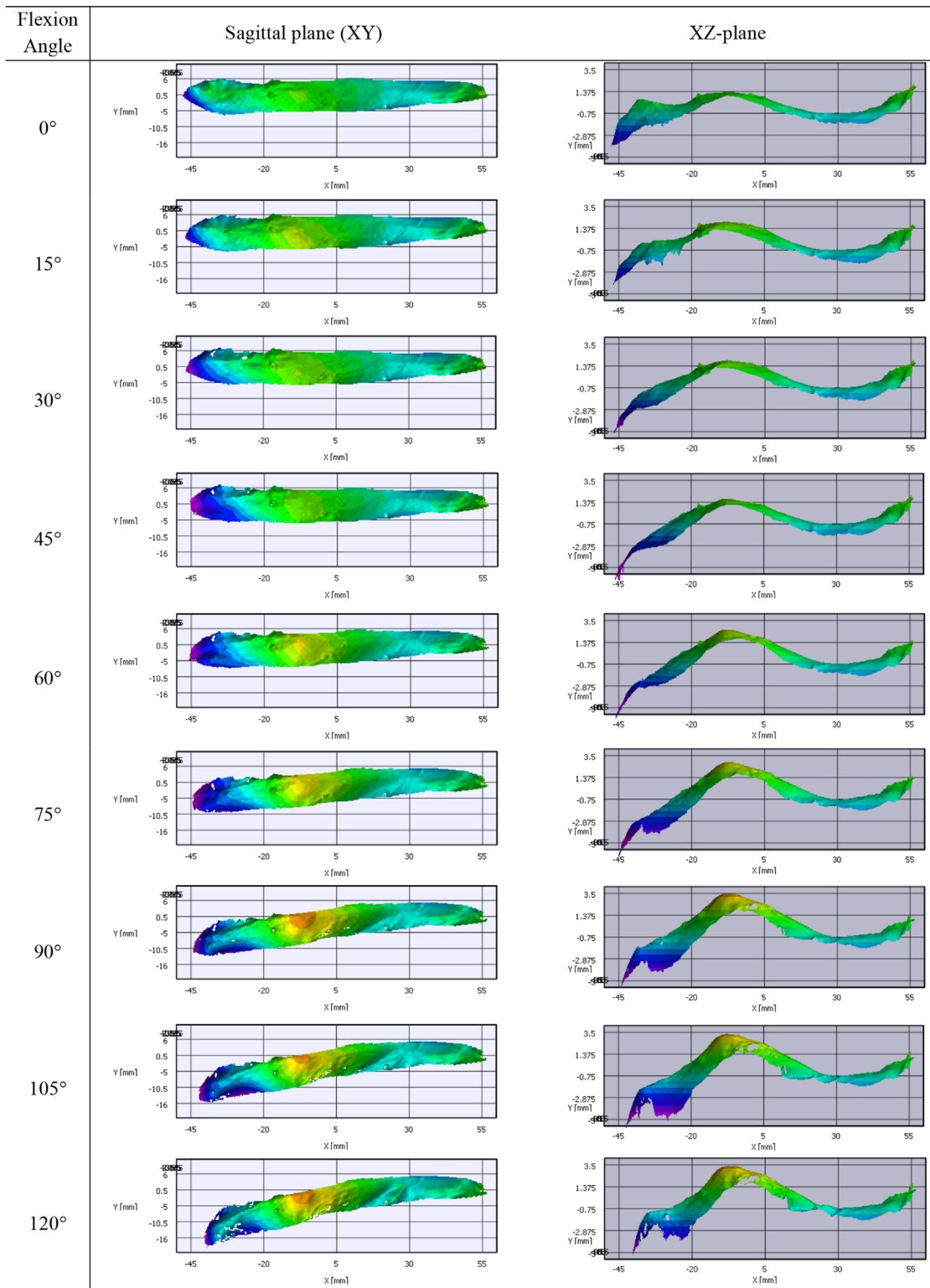


**Figure 3.** Typical example of the deformation analysis of the sMCL in the frontal (XZ) and sagittal (XY) plane through the range of motion of specimen 3. The color scale indicates the Z-coordinate.

observed, which averaged  $14^\circ$  in deep knee flexion ( $120^\circ$  flexion—Fig. 4) ( $p < 0.05$ ).

A significant amount of deformation was also observed in the frontal plane. Here, within the proximal part, a significant medialization of the proximal

tibial attachment site relative to the femoral attachment site was observed with increasing knee flexion (Fig. 2). When the 3D DIC surface map was projected on the CT reconstruction images, the most medial point in the frontal plane (maximum z-coordinate)

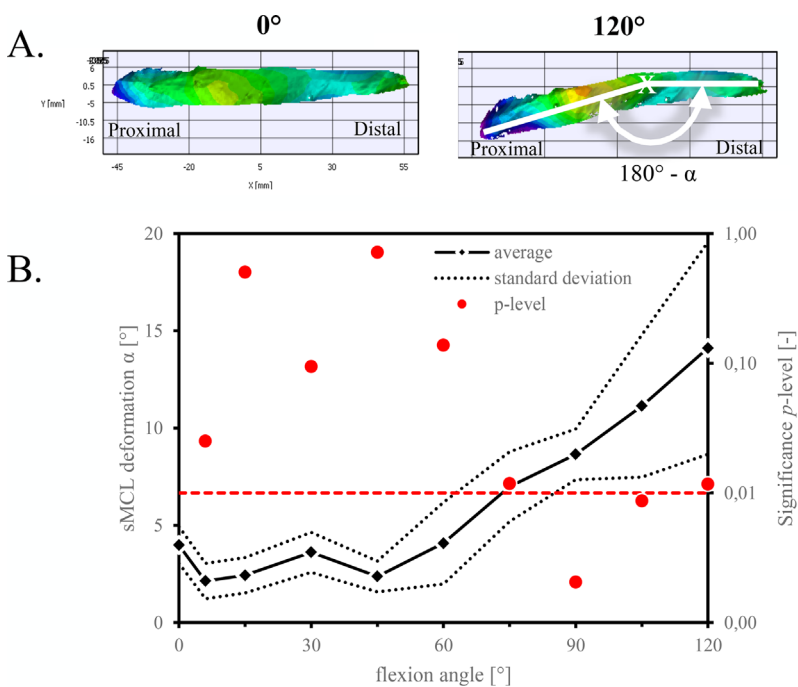


**Figure 4.** A view on the sMCL in the sagittal plane at 0° and 120° of knee flexion (A). At 0°, the sMCL was a rectangular bar. During knee flexion, this bar is progressively deformed. The deformation can be described as a rotation around the point X. This point was found to be located at the proximal tibial insertion site of the sMCL. The inclination angle  $\alpha$  as function of the flexion angle is shown in (B). A statistically significant deformation occurred at flexion angles of more than 60°.

coincided with the course of the sMCL over the proximal tibia just distal to the joint line (Fig. 3).

### Strain Analysis

First, the longitudinal strain in the central part of the whole sMCL from the femoral to distal tibial attachment was analyzed (Fig. 5). A typical example of a 3D strain map of the sMCL is shown in the supplementary material. From full extension to 30° of flexion, a slackening of on average  $-0.8\%$  was observed with progressive knee flexion. Between 15° and 90° of knee flexion, the average strain in the sMCL remained below  $0.3\%$ . In deep flexion (90° to 120°), a further slackening of the sMCL of on average  $-1.0\%$  was seen until a total

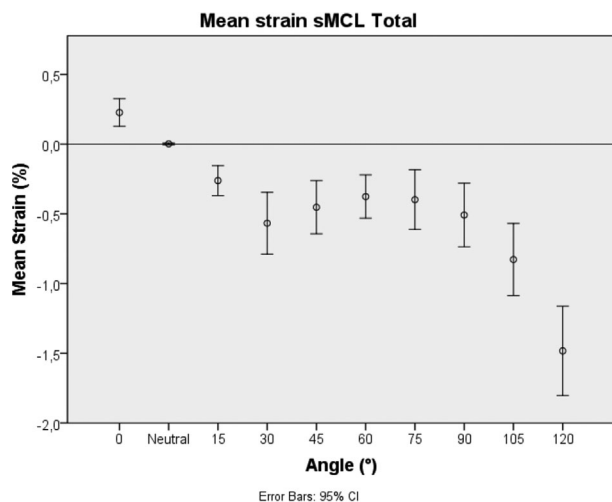


**Figure 5.** Longitudinal strain in the central part of the sMCL from proximal femoral to distal tibial insertion site during the range of motion for all 5 specimens. Means are represented with a 95% confidence interval.

slackening of on average  $-1.5\%$  was seen compared to the neutral position. During the whole range of motion, the maximum strain over the sMCL was on average  $-1.7\%$ . The latter is obtained by comparing the average strain at 0° knee flexion ( $+0.2\%$ ) with the average strain at 120° knee flexion ( $-1.5\%$ ).

Next, a subdivision of the sMCL in three regions was created (Fig. 6) and the longitudinal strain in each region was analyzed. Significant regional inhomogeneity was observed. The strain in the proximal part of the sMCL (region A) was significantly different from the strain in the middle (region B) and the distal portion (region C) at any point from 15° to 120° of knee flexion (Fig. 5) ( $p < 0.05$ ). The highest strains (average  $3.7\%$ , SD  $1.5\%$ ) were seen in this proximal part of the sMCL at 90° of flexion. The strains in the middle and distal part were not significantly different from each other or from the strain in the central part sMCL (Fig. 6).

For all specimens, the strain accumulated over the entire surface of the sMCL was the highest at full extension. The accumulated strain gradually decreased with knee flexion and was the lowest in deep flexion (Fig. 7).

### DISCUSSION

The most important finding from this study was that the sMCL did not behave as a homogeneous rigid bar but was significantly deformed in three planes throughout the range of motion. As a result, the strain in the proximal part of the sMCL was significantly different from the strain in the middle and distal portion. LaPrade et al.<sup>17</sup> recently described the sMCL and its insertion sites in a detailed quantitative way. The quantitative description of the insertion sites of the ligament opened the door for a better biomechanical

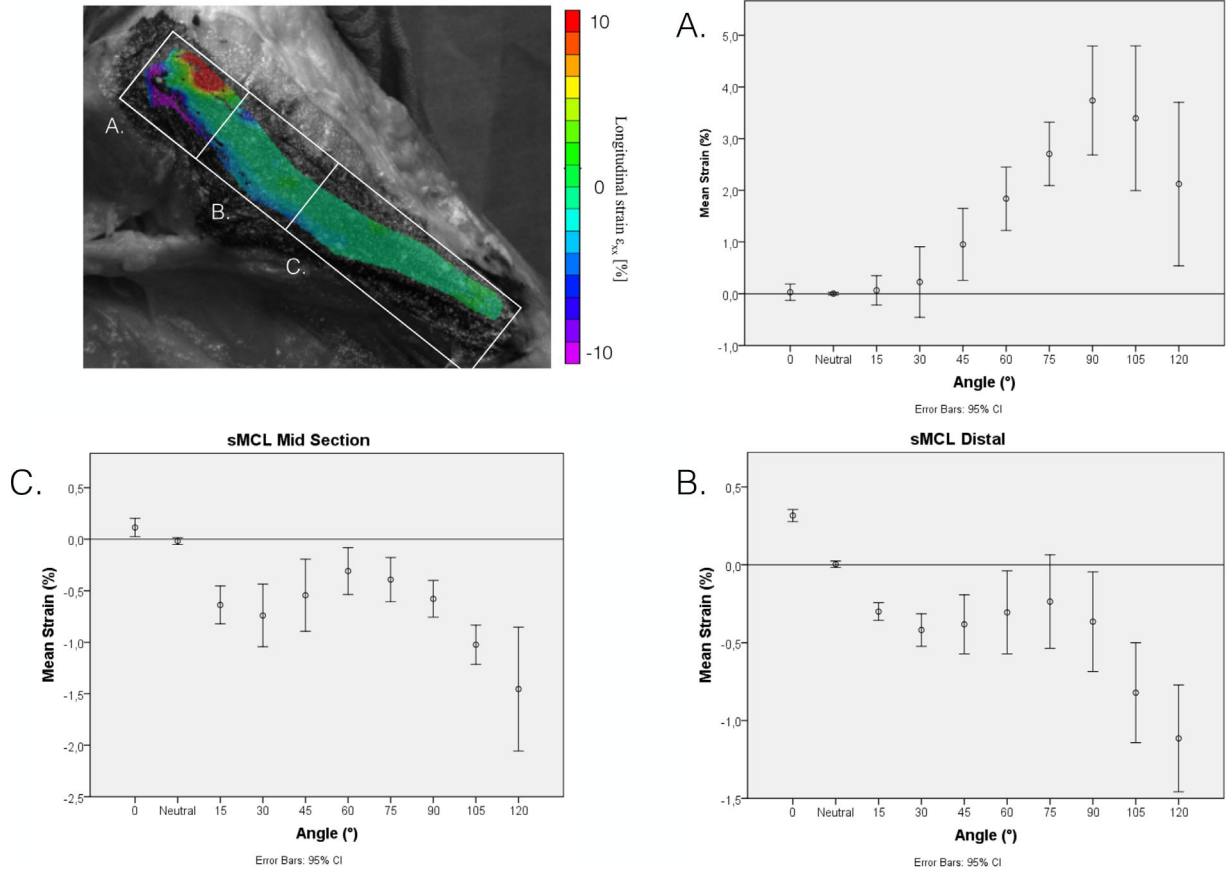


**Figure 6.** Regional (A: proximal, B: middle, C: distal) strain distribution in the sMCL according to the flexion angle for the five specimens. The mean values are represented with the 95% confidence interval. Positive values indicate lengthening, negative values shortening. Significantly higher strains are noted in the proximal region.

understanding of the ligament’s function. This knowledge is crucial for sMCL repair and reconstruction techniques. From an anatomical point of view, the sMCL was long considered to be a rectangular homogenous

structure. This conventional anatomical description describes the sMCL as a simplified two-dimensional structure that is only situated in the sagittal plane. The current study adds a new perspective to the understanding of the anatomy of the sMCL by defining the anatomy three dimensionally and analyzing it during motion. Apart from the rectangular appearance in the sagittal plane, it was found that a rather S-shaped morphology defines the sMCL in the coronal plane. Furthermore, it was found that in both the sagittal and frontal plane, significant deformation of the sMCL occurred with knee flexion. The sMCL can therefore no longer be looked at as a rigid rectangular bar. The most important deformation was found in the sagittal plane where a rotation of the distal part of the sMCL relative to the proximal part occurred with the center of rotation being the proximal sMCL insertion site. This finding is of critical importance for sMCL reconstruction techniques. Only fixing the graft at the distal insertion site on the tibia but not on the proximal tibial location could cause laxity in flexion. This is a consequence of the fact that the femoral and distal tibial insertion sites approach each other with increasing knee flexion (Fig. 8). Reconstruction of the proximal tibial insertion site of the sMCL is therefore

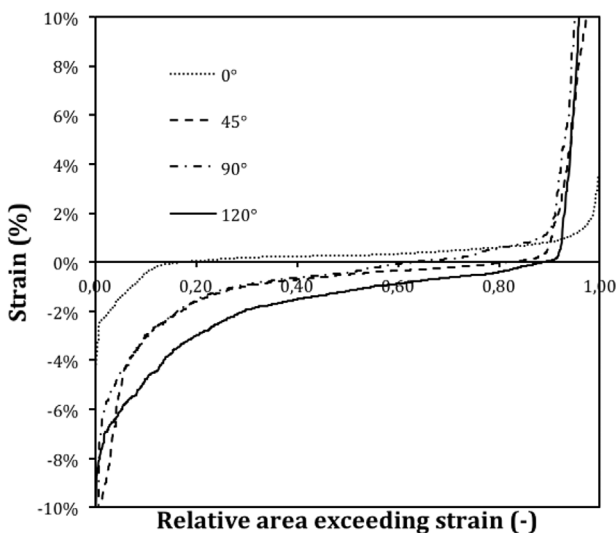


**Figure 7.** Cumulative strain distribution in the sMCL at different flexion angles in specimen 6.

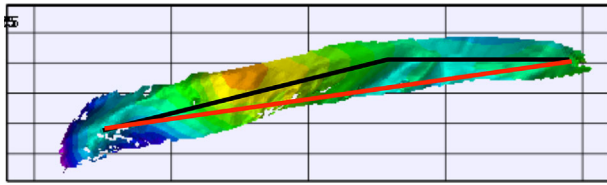


**Figure 8.** The distance between the femoral and distal tibial insertion site of the sMCL (in red) is smaller in flexion than in extension as both insertion sites approach each other. Only fixing the graft at the distal insertion site on the tibia but not on the proximal tibial location would therefore cause laxity in flexion.

crucial to maintain its isometry and thus stability throughout the whole range of motion.<sup>7,8</sup>

The second most important finding of this study was that the strain in the sMCL was inhomogeneously distributed over its surface with the strain in the proximal part near the sMCL insertion site being the highest. This observation can be directly related to the in vivo failure pattern of the sMCL. Tears of the sMCL are most frequently found near the femoral insertion site. They occur with the knee in slight flexion. At full extension, more than 50% of the restraint against valgus force is provided by the MCL.<sup>1,23,24</sup> The posterior oblique ligament (POL), ACL, and posteromedial capsule are responsible for the majority of the remaining restraint. At 25° of knee flexion however, more than 70% of the restraint against valgus is provided by the MCL, making it more vulnerable for injury.<sup>1,23,24</sup> At this flexion angle, the strain in the proximal part of the sMCL was significantly higher than in the other parts (Fig. 6). Due to this “preload” strain in the proximal part, a pathologic elongation caused by an external valgus force is more likely to cross the damage threshold first in this region and cause structural defects.

A possible explanation for the higher strains in this region can be found in the fact that the center of rotation of the knee in the femur coincides with the insertion site on the sMCL on the femur.<sup>25</sup> As the femoral insertion site of the sMCL is not a point but a surface area of on average 94.1 mm<sup>2</sup>, part of the sMCL fibers at the insertion site will be located anterior to the axis of rotation and part of the fibers posterior to it.<sup>17</sup> This implies a sort of wrapping around the axis of rotation of the proximal sMCL fibers when the knee is flexed.<sup>12</sup> This will cause elongation of the anterior fibers and slackening of the posterior ones. This hypothesis was confirmed by our findings showing high strains in the anterior proximal part of the sMCL with progressive knee flexion and lower strains in the posterior proximal part. We theorize that previous studies fail to detect these differences because of a low spatial resolution of the used measurement method or investigation of only a part of the sMCL. Because the surface area of the proximal part is relatively small, its effect on the total strain is small and is easily missed.

This regional strain being significantly different from the overall strain was suggested by other studies although the spatial resolution of the measurement

methods was fairly low and did not allow for regional strain analysis.<sup>11</sup> The inhomogeneous, non-linear and anisotropic nature of biological tissue explains part of this observation. From a pathogenic point of view, the sMCL therefore cannot be thought of as a single homogenous unit. Local strains stayed local and were not propagated across the whole ligament. Several factors might explain this observation. The bone geometry was one factor. As demonstrated in Figure 1, the sMCL is not a linear structure. The shape of the distal femur, the medial epicondyle and the proximal tibial plateau determine the 3D surface morphology of the sMCL, which had important variability in the three planes. Knee motion will therefore affect the different parts of the sMCL differently. Second, from a biologic point of view, a ligament is known to be an inhomogeneous structure, which can show important regional variation in collagen bundle branching, fiber size and the amount of ground substance. These factors all affect local stiffness and strain. Third, interactions with the posterior oblique ligament are likely to affect the proximal and distal part of the sMCL differently because the fiber orientation is different in those parts. One of the advantages of our study was that no dissection of the sMCL was performed. The ligament was left untouched in its native bed, thereby preserving any existing connection with surrounding structures and thus mimicking the in vivo situation. Finally, tibiofemoral motion, both rotational and translational might affect the different parts of the sMCL differently.

A third important finding of this study was that, from a biomechanical point of view, the sMCL was confirmed to be a nearly perfect isometric ligament. According to the existing literature, a ligament is considered isometric when the strain in the ligament is less than 2% during the range of motion.<sup>10,13</sup> Our data confirm these findings but with greater accuracy. When considered in its central portion between 15° and 90° of knee flexion, the strain in the sMCL fibers remained below 0.3%. Therefore, the central fibers of the sMCL did indeed prove to be near perfectly isometric, with limited strain (<2%) throughout the whole range of motion. This finding is important for sMCL reconstruction techniques. Only a perfect anatomic restoration of the insertion sites of the sMCL on the femur and tibia will be able to reproduce this isometry and thus provide the adequate stability throughout the range of motion. Even small deviations will cause an anisometric graft with ligament laxity or elongation with knee flexion, depending on the position of the graft relative to the anatomic insertion site.<sup>9,26</sup> These findings might also have important implications toward postoperative rehabilitation protocols after sMCL reconstruction. The fact that knee motion between 15° and 90° caused minimal strain in the sMCL might suggest that early passive range of motion in physical therapy postoperatively should have little risk of stretching a graft out.

Our study has several limitations. First, the fact that only five specimens were available for analysis

after exclusion of one specimen due to poor speckle tracking quality. However, the high resolution and accuracy of the measurement technique allowed us to draw significant conclusions. A second limitation was the fact that the knee was loaded in a static way. Further research is needed to enable extrapolation of these data to the dynamic in vivo situation. A third limitation was the fact that the analysis was limited to the properties of the superficial layer of a tissue sample. However, our data are consistent with previous studies using invasive measurement methods.

## CONCLUSION

A significant deformation of the sMCL was observed in three planes during knee flexion. This deformation generated high strains near the sMCL femoral insertion site and might explain why most lesions in clinical practice are seen in this region. The deformation also has important implications for sMCL reconstruction techniques. Fixing a graft on both the proximal and distal tibial insertion sites is critical to maintain the isometric behavior of the sMCL and maintain stability throughout the whole range of motion. The fact that knee motion between 15° and 90° caused minimal strain in the sMCL might suggest that early passive range of motion in physical therapy postoperatively should have little risk of stretching a graft out in the case of an anatomical reconstruction.

## AUTHORS' CONTRIBUTIONS

Dr. T. Luyckx and Mr. M. Verstraete have contributed equally to this article and share first authorship. T.L. conceived of the study. T.L., M.V., and K.D. carried out all experiments and drafted the manuscript. J.V. and C.V.D.S. also conceived of the study, and participated in its design and coordination and helped to draft the manuscript. All authors read and approved the final manuscript.

## REFERENCES

- Griffith CJ, LaPrade RF, Johansen S, et al. 2009. Medial knee injury: part 1, static function of the individual components of the main medial knee structures. *Am J Sports Med* 37:1762–1770.
- Wijdicks CA, Griffith CJ, Johansen S, et al. 2010. Injuries to the medial collateral ligament and associated medial structures of the knee. *J Bone Joint Surg Am* 92:1266–1280.
- Miyasaka KC, Daniel DM, Stone ML, et al. 1991. The incidence of knee ligament injuries in the general population. *Am J Knee Surg* 4:3–8.
- Daniel D, Pedowitz R, O'Connor J, et al. 2003. *Daniel's knee injuries: ligament and cartilage structure, function, injury and repair*, 2nd ed. Philadelphia: Lippincott Williams and Wilkins.
- Lee JI, Song IS, Jung YB, et al. 1996. Medial collateral ligament injuries of the knee: ultrasonographic findings. *J Ultrasound Med* 15:621–625.
- Kawada T, Abe T, Yamamoto K, et al. 1999. Analysis of strain distribution in the medial collateral ligament using a photoelastic coating method. *Med Eng Phys* 21:279–291.
- Coobs BR, Wijdicks CA, Armitage BM, et al. 2010. An in vitro analysis of an anatomical medial knee reconstruction. *Am J Sports Med* 38:339–347.
- Wijdicks CA, Michalski MP, Rasmussen MT, et al. 2013. Superficial medial collateral ligament anatomic augmented repair versus anatomic reconstruction: an in vitro biomechanical analysis. *Am J Sports Med* 41:2858–2866.
- Feeley BT, Muller MS, Allen AA, et al. 2009. Biomechanical comparison of medial collateral ligament reconstructions using computer-assisted navigation. *Am J Sports Med* 37:1123–1130.
- Victor J, Wong P, Witvrouw E, et al. 2009. How isometric are the medial patellofemoral, superficial medial collateral, and lateral collateral ligaments of the knee? *Am J Sports Med* 37:2028–2036.
- Arms S, Boyle J, Johnson R, et al. 1983. Strain measurement in the medial collateral ligament of the human knee: an autopsy study. *J Biomech* 16:491–496.
- Warren LA, Marshall JL, Girgis F. 1974. The prime static stabilizer on the medial side of the knee. *J Bone Joint Surg Am* 56:665–674.
- Ghosh KM, Merican AM, Iranpour F, et al. 2012. Length-change patterns of the collateral ligaments after total knee arthroplasty. *Knee Surg Sports Traumatol Arthrosc* 20:1349–1356.
- Wren TAL, Yerby a S, Beaupr GS, et al. 2001. Mechanical properties of the human Achilles tendon. *Clin Biomech (Bristol, Avon)* 16:245–251.
- Gardiner JC, Weiss JA, Rosenberg TD. 2001. Strain in the human medial collateral ligament during valgus loading of the knee. *Clin Orthop Relat Res* 391:266–274.
- Ravary B, Pourcelot P, Bortolussi C, et al. 2004. Strain and force transducers used in human and veterinary tendon and ligament biomechanical studies. *Clin Biomech (Bristol, Avon)* 19:433–447.
- LaPrade RF, Engebretsen AH, Ly T, et al. 2007. The anatomy of the medial part of the knee. *J Bone Joint Surg Am* 89:2000–2010.
- Amis AA, Oguz C, Bull AMJ, et al. 2008. The effect of trochleoplasty on patellar stability and kinematics: a biomechanical study in vitro. *J Bone Joint Surg Br* 90:864–869.
- Farahmand F, Senavongse W, Amis AA. 1998. Quantitative study of the quadriceps muscles and trochlear groove geometry related to instability of the patellofemoral joint. *J Orthop Res* 16:136–143.
- Victor J, Labey L, Wong P, et al. 2010. The influence of muscle load on tibiofemoral knee kinematics. *J Orthop Res* 28:419–428.
- Schreier H, Orteu J-J, Sutton MA. 2009. *Image correlation for shape, motion and deformation measurements*. Boston, MA: Springer US. p 322.
- Luyckx T, Verstraete M, De Roo K, et al. 2014. Digital image correlation as a tool for three-dimensional strain analysis in human tendon tissue. *J Exp Orthop* 1:7.
- Grood E, Noyes F, Butler D, et al. 1981. Ligamentous and capsular restraints preventing straight medial and lateral laxity in intact human cadaver knees. *J Bone Joint Surg Am* 63:1257.
- Griffith CJ, Wijdicks CA, LaPrade RF, et al. 2009. Force measurements on the posterior oblique ligament and superficial medial collateral ligament proximal and distal divisions to applied loads. *Am J Sports Med* 37:140–148.
- Hollister AM, Jatana S, Singh AK, et al. 1993. The axes of rotation of the knee. *Clin Orthop Relat Res* 290:259–268.
- Feeley BT, Muller MS, Allen AA, et al. 2009. Isometry of medial collateral ligament reconstruction. *Knee Surg Sports Traumatol Arthrosc* 17:1078–1082.

## SUPPORTING INFORMATION

Additional supporting information may be found in the online version of this article at the publisher's website.